Supplementary Information for

Title: Characteristics and anatomic location of PD-1^{+}TCF1^{+} stem-like CD8 T cells in chronic viral infection and cancer

Se Jin Im[a,b,c,1,*], Rebecca C. Obeng[a,b,d,e,1], Tahseen H. Nasti[a,b], Daniel McManus[a,b], Alice O. Kamphorst[f,g], Sivaram Gunisetty[a,b], Nataliya Prokhnevska[a,h], Jennifer W Carlisle[i,j], Ke Yu[d], Gabriel L. Sica[d,j,k], Lucas E. Cardozo[l], André N.A. Gonçalves[l], Haydn T. Kissick[a,h], Helder I. Nakaya[l], Suresh S. Ramalingam[i,j,*], and Rafi Ahmed[a,b,*]

[a]Emory Vaccine Center, Emory University School of Medicine, Atlanta, GA 30322, USA
[b]Department of Microbiology and Immunology, Emory University School of Medicine, Atlanta, GA 30322, USA
[c]Department of Immunology, Sungkyunkwan University School of Medicine, Suwon 16419, Republic of Korea
[d]Department of Pathology and Laboratory Medicine, Emory University School of Medicine, Atlanta, GA 30322, USA
[e]Department of Pathology, Case Western Reserve University School of Medicine, Cleveland, OH 44106, USA
[f]Department of Immunology and Immunotherapy, Lipschultz Precision Immunology Institute, Tisch Cancer Institute, Icahn School of Medicine at Mount Sinai, New York, NY 10029, USA
[g]Department of Oncological Sciences, Lipschultz Precision Immunology Institute, Tisch Cancer Institute, Icahn School of Medicine at Mount Sinai, New York, NY 10029, USA
[h]Department of Urology, Emory University School of Medicine, Atlanta, GA 30322, USA
[i]Department of Hematology and Medical Oncology, Emory University School of Medicine, Atlanta, GA 30322, USA
[j]Winship Cancer Institute, Emory University School of Medicine, Atlanta, GA 30322, USA
[k]Department of Pathology, University of Pittsburgh School of Medicine, Pittsburgh, PA 15213, USA
[l]Hospital Israelita Albert Eisnstein, Sao Paulo 05652, Brazil

[1]S.J.I. and R.C.O. contributed equally to this work.
[*]Co-corresponding authors

[*]Corresponding author: Se Jin Im, Ph.D.

Department of Immunology, Sungkyunkwan University School of Medicine
2066 Seobu-ro, Jangan-gu, Suwon 16419, Republic of Korea
Phone: +82-31-299-6125
Email: sejinim@skku.edu

*Corresponding author: Suresh S. Ramalingam, MD.
Department of Hematology and Medical Oncology, Emory University School of Medicine
1365 Clifton Rd Rm G211, Atlanta GA, 30322, US
Phone: +1-404-778-1900
Email: ssramal@emory.edu

*Corresponding author: Rafi Ahmed, Ph.D.
Emory Vaccine Center, Emory University School of Medicine
1510 Clifton Rd Rm G211, Atlanta GA, 30322, USA
Phone: +1-404-727-3571
Email: rahmed@emory.edu

This PDF file includes:

Supplementary text
Figs. S1 to S3
Tables S1 and S2
References for SI reference citations

Supplementary Information Text

SI Materials and Methods

Mice and chronic LCMV infection

Six- to eight-week-old female C57bl/c mice, Balb/c mice, and CD45.1 congenic mice were purchased from Jackson Laboratory. For chronic LCMV infection, mice were infected with $2x10^6$ pfu LCMV Cl-13 intravenously after transient CD4 T cell depletion with 500 µg GK1.5 anti-CD4 antibody intraperitoneally. All animal experiments were performed in accordance with Emory University Institutional Animal Care and Use Committee.

Collagenase treatment for spleens

Spleens isolated from mice chronically infected with LCMV were divided into two parts. One half was used to isolate lymphocytes by mechanical disruption and the other half was cut into small pieces and treated with Collagenase IV (150 U/ml) for 1 hour at 37ºC with shaking. Then, splenocytes were isolated as described previously(1).

Mouse tumor cell lines, inoculation, and TIL isolation

Mouse skin melanoma B16F10-GP ($5x10^5$), lung carcinoma LLC1-GP ($5X10^5$), prostate adenocarcinoma TRAMP-C2 ($5X10^5$), and colon carcinoma CT26 ($5x10^5$) cells suspended in 25% Matrigel Matrix (Corning)/RPMI were injected on the right flank (day 0). B16F10-GP, LLC1-GP, and TRAMP-C2 were inoculated into C57bl/6 mice and CT26 was inoculated into Balb/c mice. Tumors were harvested in RPMI media including 5% FCS when the tumors reached the size of about $1cm^2$ area, cut into small pieces and digested for 1 hour with Collagenase IV (150 U/mL) and DNase (20 µg/ml) at 37ºC with shaking. Single cell suspension of TILs was isolated by 44%/67% Percoll gradient centrifugation.

Human cancer patient samples

Primary and metastatic tumors in lung tissues were obtained from 19 patients with stage I-IV disease who underwent surgical resection as standard care. None of the patients received checkpoint inhibitors prior to surgery. ICI was not being used routinely at that time. Seven of the samples were collected between 2014 and 2016. Of those samples, five were from stage 2-3 tumors, one was stage 4, and tumor stage was not available for one sample. The rest of the samples was collected in 2018 and consisted of 3 metastatic tumors to the lung and 5 primary lung tumors that were between stages 1 and 3. Patients were consented for tissue and blood collection under an Emory University Winship Cancer Institute tissue collection protocol, in accordance with the Emory University Institutional Review Board. Tumors were harvested in cold L-15 Leibovitz media (Hyclone), cut into small pieces and digested for 1 hour with an enzyme cocktail of Collagenase I (125 mg/L), Collagenase II (125 mg/L), Collagenase IV (125 mg/L), DNase I (50 mg/L), and Elastase (50 mg/L) (Worthington) at 37ºC with shaking. Lymphocytes were isolated by 44%/67% Percoll gradient centrifugation. Peripheral blood mononuclear cells were isolated according to standard protocol. Fractions of the single cell suspensions were stained for immediate analysis by flow cytometry and the remaining cells were frozen for subsequent analyses.

Flow Cytometry and antibodies

Flow cytometric analysis was performed on a FACS Canto II or LSR II (BD Biosciences). FACS data were analyzed with FlowJo software (TreeStar).

Murine samples: Single cell suspension were stained with anti-CD8a (53.6.7), -CD4 (GK1.5), -CD19 (1D3), -PD-1 (RMP1-30 or 29F.1A12), -Tim-3 (RMT3-23), -CD73 (TY/11.8), -2B4 (m2B4(B6)458.1), -CXCR5(L138D7), -Ly5.2(104), and -Ki-67 (B56) from BD, eBioscience or BioLegend; Granzyme B (GB12) from Invitrogen; TCF1 (C63D9) from Cell Signaling Technologies (CST). LCMV MHC class I tetramers were prepared and used as previously described(2). CT26-specific AH1 MHC class I tetramers were purchased from MBL International Corporation. Live/Dead cell discrimination was performed using Aqua Dead Cell Stain Kit (Life Technology). Intracellular staining for Granzyme B and for Ki-67 and TCF1 was performed with Cytofix/Cytoperm kit (BD Bioscience) and Foxp3 Staining Buffer Set (eBioscience)

according to manufacturer's instruction, respectively.

Human samples: Single cell suspension were stained with anti-CD8a (RPA-T8), -CD4 (RPA-T4), -CD3 (SK7), -PD-1 (EH12.2H7), -CD28 (CD28.2), -CD39 (A1), -Granzyme B (GB11), and -Ki-67 (B56) from BD, eBioscience or BioLegend; -Tim-3 (344823) from R&D systems; -TCF1(C63D9) from CST. Dead cells were excluded by gating out cells positive for Aqua Dead Cell Stain Kit (Life Technology). Intracellular staining for Ki-67 and TCF1 was performed with Foxp3 Staining Buffer Set (eBioscience) according to manufacturer's instruction.

Cell sorting

Cell sorting was performed on a FACS Aria II (BD Biosciences) for microarray analysis, RNA-seq, and transfer experiments of mouse samples and for RNA-seq analysis of human samples. From B16F10-GP bearing mice, stem-like (Tim-3$^-$2B4$^-$ PD-1$^+$) and exhausted (Tim-3$^+$2B4$^+$ PD-1$^+$) CD8 T cells were isolated between day 17 and day 19 post inoculation. Stem-like (Tim-3$^-$CD28$^+$ PD-1$^+$) and exhausted (Tim-3$^+$ PD-1$^+$) human CD8 T cells were sorted from frozen TIL samples isolated from NSCLC patients.

RNA isolation, microarray analysis, and RNA-seq

RNA from FACS sorted cells was purified by Allprep DNA/RNA micro kit (QIAGEN). RNA isolated from mouse TILs was hybridized to Affymetrix mouse 430 2.0 arrays (Emory University, Genomics Core Facility). Raw data (CEL files) were normalized by RMA using Affy R package. For RNA-seq, RNA was processed for sequencing using the Clontech smartseq V2 kit. Libraries were prepared using the Illumnia Nextera kit, and sequenced on a Hiseq 3000. Sequence data was aligned using HiSat2(3), and differential gene expression was determined using DeSeq2(4).

Gene Set Enrichment Analysis was run for each cell subset in pre-ranked list mode with 1,000 permutations (nominal p-value cutoff < 0.01). Differentially expression analysis was performed using EdgeR package(5) and genes were defined as differentially expressed based on a FDR cutoff < 0.05 and $\log_2$ fold-change cutoff > 1. The Enrichment Map Visualization of GSEA analysis was created using Cytoscape with

significant gene sets (p-value cutoff < 0.005 and FDR Q-value cutoff < 0.1).

Adoptive cell transfer, and Cl13 rechallenge

Twenty thousand sorted stem-like CD8 T cells and forty thousand sorted exhausted CD8 T cells were transferred into naive CD45.1 congenic mice. Both donor stem-like and exhausted CD8 T cells contained one thousand GP33/GP276-specific CD8 T cells. One day after the transfer, recipient mice were challenged with $2x10^6$ pfu LCMV Cl-13 strain intravenously.

Intravascular labeling

For intravascular labeling, 3 μg of BV421-conjugated anti-CD8α antibody (BioLegend) was injected intravenously into chronically infected mice. Three minutes after the injection, splenocytes were isolated and stained *ex vivo* as described previously(6).

Multiplex immunohistochemistry

Seven-color multiplex immunohistochemistry was performed using the OPAL Polaris and OPAL Tumor Immunology kits (Akoya Biosciences). Four to five-micron sections of formalin-fixed paraffin-embedded primary and metastatic tumors from surgical resections of the lungs of patients were deparaffinized, hydrated, and stained manually with anti-CD3 (clone F7.2.38, Dako), CD4 (clone 3H8, Biolegend), CD8 (clone C8/144B, eBiosciences), CD20 (clone L26, Akoya Biosciences kit), TCF-1 (clone C63D9, CST), PD-1 (clone D2W2J, CST), and cytokeratin (clone AE1/3, Dako) antibodies. Heat induced epitope retrieval (HIER) in EDTA (pH 9) or citrate (pH 6) buffer was performed prior to blocking the tissues and staining with the primary antibodies. The sections were sequentially stained with each primary, HRP-conjugated secondary antibody, tyramide signal amplification, and OPAL fluorophore according manufacturer's instructions. OPAL 480, 520, 540, 570, 620, 650, 690, and 780 dyes were used. The sections were counterstained with spectral DAPI (Akoya Biosciences). The stained slides were annotated using phenoChart 1.0.12 (Akoya Biosciences) and InForm software (Akoya Biosciences). The slides were then

imaged and scanned using the Vectra Polaris multispectral imaging system or the Leica SP8 Confocal microscope.

Image analysis

For carcinomas, the tumor areas on each slide were identified using the cytokeratin marker. Morphologic, DAPI, and nuclear features were used to identify tumor parenchyma for the metastatic melanoma samples. The stroma within the tumor was differentiated from the tumor parenchyma using the cytokeratin marker and morphologic features. For the analysis of specific areas within and around the tumor (ITL, iTLS, pTLS, and aTLS), one to 4 images of each specific area were manually selected, acquired on a Leica SP8 microscope, processed using ImageJ V2.0.0-rc-69/1.52p (NIH), and manually quantified. For spatial map views and analysis, random areas of high-resolution whole slide scanned images that included TLSs were first annotated in PhenoChart v1.0.12 and then analyzed with the inForm2.4.8 software. Tumor and stroma areas were identified using cytokeratin as a marker for tumor and adaptive cell segmentation was accomplished based on nuclear DAPI and membranous CD20 staining. Fifteen to 35 cells from the phenotypes of the immune cells of interest were manually selected and used to train the software for automated phenotype analysis. Six to 22 representative regions per tumor sample were analyzed for total areas of 3.8 to 14 mm^2. The data was processed in R studio using phenoptr (v0.2.5) and phenoptrReports (v0.2.6) (Akoya Biosciences).

Statistical analysis

All experiments were analyzed using Prism 7 (GraphPad Software). Statistical differences were assessed using a two-tailed unpaired or paired Student's t-test. P values of <0.05 and <0.01 indicated the significant difference between relevant groups.

Supplementary Figure 1

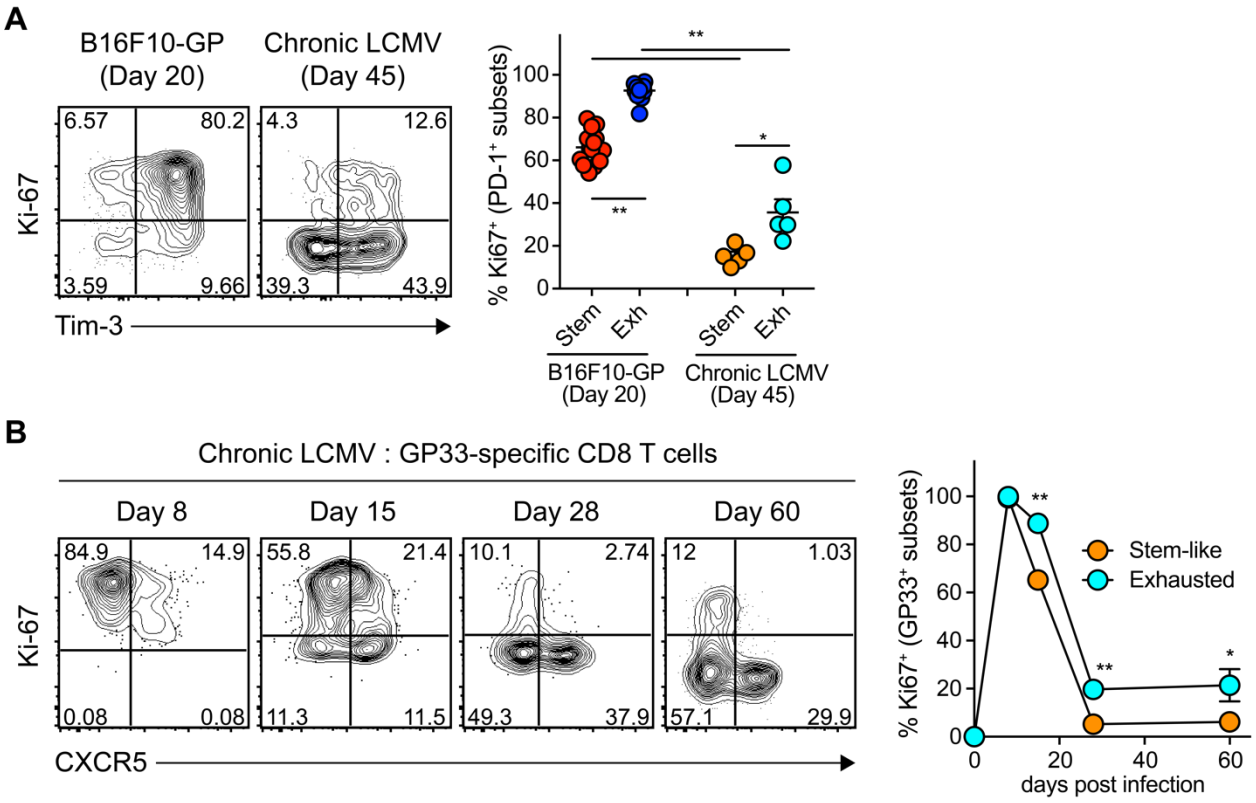

Supplementary Figure 1. Kinetics of Ki-67 expression in exhausted CD8 T cell subsets. (A) Representative FACS plots and the frequency of Ki-67$^+$ cells among PD-1$^+$ CD8 T cell subsets at the indicated time points in the tumors and spleen of tumor-bearing mice and chronically infected mice with LCMV, respectively. (B) Representative FACS plots and the kinetics of Ki-67$^+$ cells among LCMV GP33-specific CD8 T cell subsets in the spleen of chronically infected mice. Data were combined results or representative of three independent experiments (n=4-5 / experiment). Graph shows the mean and s.e.m. Student's t-test, where ** $p<0.01$; * $p<0.05$.

Supplementary Figure 2

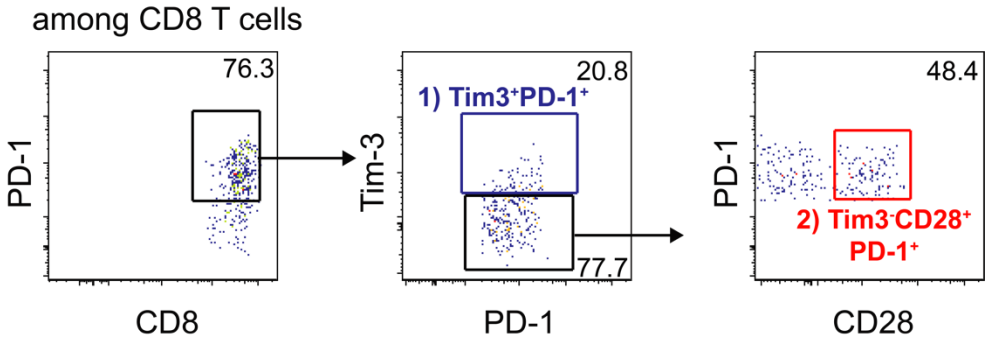

Supplementary Figure 2. Gating strategies to isolate two CD8 TIL subsets from NSCLC tumors. Stem-like Tim-3^{-}CD28^{+} PD-1^{+} and terminally differentiated Tim-3^{+} PD-1^{+} CD8 T cells were isolated from six NSCLC patients.

Supplementary Figure 3

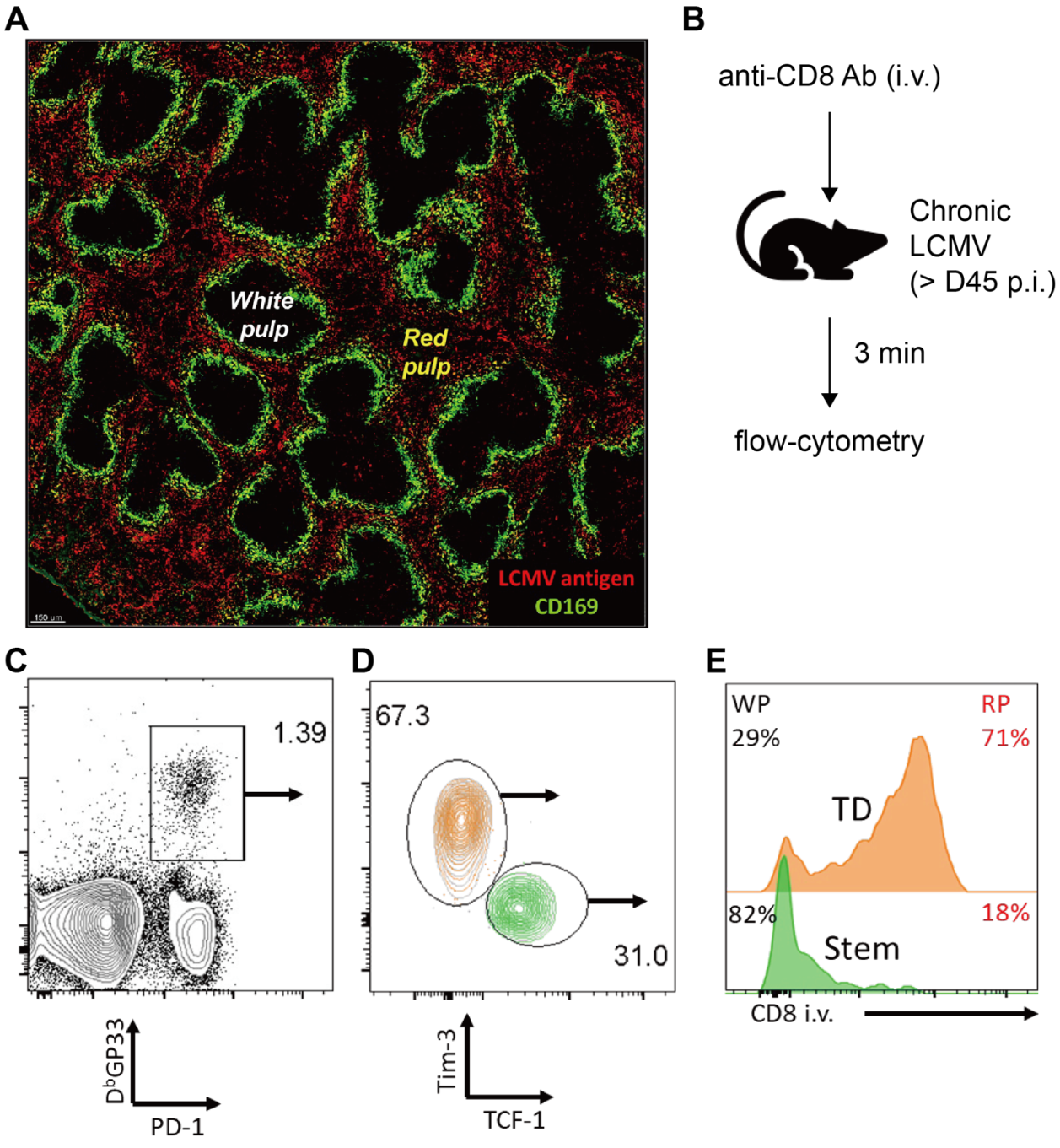

Supplementary Figure 3. Stem-like CD8 T cells compartmentalize to the splenic white pulp during chronic viral infection. (A) Representative image of viral antigen distribution in chronic LCMV-infected spleen (> day 45 p.i.). Splenic sections were stained for LCMV antigen (red) and CD169 (green). (B)

Chronically infected mice (> day 45 p.i.) were injected with 3 μg anti-mouse CD8α and sacrificed 3 mins later. (C-D) Representative flow plots showing the frequency of LCMV GP33-specific CD8 T cells (C) and their stem-like ($TCF1^{+}Tim\text{-}3^{-}$) and terminally differentiated ($TCF1^{-}Tim\text{-}3^{+}$) subpopulations (D). (E) Representative histogram showing intravascular label on LCMV-specific stem-like (Stem) and terminally differentiated (TD) CD8 T cell subsets. Data are representative of two independent experiments (n=3-5 per experiment).

Table S1. Clinical characteristics of NSCLC patients on this study

	n = 16
Median age at time of resection (range)	65 (42-83)
Sex, n (%)	
Male	11 (69%)
Female	5 (31%)
Race, n (%)	
Caucasian	12 (75%)
African-American	4 (25%)
Smoking status, n (%)	
Former	11 (69%)
Current	4 (25%)
Never	1 (6%)
Histology, n (%)	
Adenocarcinoma	7 (44%)
Squamous cell carcinoma	6 (38%)
Carcinoid	2 (12%)
Mixed Histology (Adenocarcinoma and large cell neuroendocrine)	1 (6%)
Pathologic stage at time of resection, n (%)	
I	5 (31%)
II	6 (38%)
III	4 (25%)
IV*	1 (6%)

* wedge biopsy to confirm bilateral disease

Table S2. Temporal patterns of PD-1, TCF1, and Ki-67 expression in chronic LCMV infection, murine tumor, and human tumor

a. Chronic LCMV infection

T sell subset	Marker	Time after infection			
		Day 8	Day 15	Day 28	> Day 60
Stem-like	PD-1	High	High	High	High
	TCF1	Pos	Pos	Pos	Pos
	Ki-67	High	Intermediate	Low	Low
*Terminally differentiated	PD-1	High	High	High	High
	TCF1	Neg	Neg	Neg	Neg
	Ki-67	High	High	Intermediate	Intermediate / Low

b. Murine Tumor

T sell subset	Marker	Time after cancer
		Day 19
Stem-like	PD-1	High
	TCF1	Pos
	Ki-67	Intermediate
*Terminally differentiated	PD-1	High
	TCF1	Neg
	Ki-67	High

c. Human Tumor

T sell subset	Marker	Time after cancer
		Months/Years
Stem-like	PD-1	High
	TCF1	Pos
	Ki-67	Low
*Terminally differentiated	PD-1	High
	TCF1	Neg
	Ki-67	Intermediate / Low

*The TCF1^{-}Tim-3^{+} PD-1^{+} “terminally differentiated” CD8 T cell population consists of a transitory effector-like subset and the exhausted CD8 T cell subset. These two subsets can be distinguished by the expression of CD101 and CX3CR1. Only the transitory CD8 T cell subset (CD101^{-}CX3CR1^{+}) shows proliferation (Ki-67^{+}) whereas the exhausted

CD8 T cell subset ($CD101^{+}CX3CR1^{-}$) has lost the ability to proliferate ($Ki\text{-}67^{-}$). The relative proportions of these two subsets are temporally regulated. At the early time points (first 2-3 weeks) there are very few end-stage exhausted CD8 T cells and the majority of the $PD\text{-}1^{+}Tim\text{-}3^{+}$ are the effector-like CD8 T cells and are proliferating. However, at later stages of the chronic infection (> day 60), the majority of the virus-specific CD8 T cells are the exhausted CD8 T cell subset that has lost the ability to divide. Upon PD-1 blockade, there is a new pool of effector-like CD8 T cells generated from the $PD\text{-}1^{+}$ $TCF1^{+}$ stem-like CD8 T cells [Refs:19 and 22].

References

1. E. J. Wherry, J. N. Blattman, K. Murali-Krishna, R. van der Most, R. Ahmed, Viral persistence alters CD8 T-cell immunodominance and tissue distribution and results in distinct stages of functional impairment. *J Virol* **77**, 4911-4927 (2003).
2. K. Murali-Krishna *et al.*, Counting antigen-specific CD8 T cells: a reevaluation of bystander activation during viral infection. *Immunity* **8**, 177-187 (1998).
3. D. Kim, B. Langmead, S. L. Salzberg, HISAT: a fast spliced aligner with low memory requirements. *Nat Methods* **12**, 357-360 (2015).
4. M. I. Love, W. Huber, S. Anders, Moderated estimation of fold change and dispersion for RNA-seq data with DESeq2. *Genome Biol* **15**, 550 (2014).
5. D. J. McCarthy, Y. Chen, G. K. Smyth, Differential expression analysis of multifactor RNA-Seq experiments with respect to biological variation. *Nucleic Acids Res* **40**, 4288-4297 (2012).
6. K. G. Anderson *et al.*, Intravascular staining for discrimination of vascular and tissue leukocytes. *Nat Protoc* **9**, 209-222 (2014).